JGR Biogeosciences

RESEARCH ARTICLE
10.1029/2023JG007900

Seasonal Variation and Key Controls of Groundwater Ammonium Concentrations in Hypoxic/Anoxic Riparian Sediments

Matthew G. Sena[1], Marc Peipoch[2], Bisesh Joshi[3], Md. Moklesur Rahman[1], Erin Peck[1], Arthur J. Gold[4], Jinjun Kan[2], and Shreeram Inamdar[1]

[1]Department of Plant & Soil Sciences, University of Delaware, Newark, DE, USA, [2]Stroud Water Research Center, Avondale, PA, USA, [3]Water Science and Policy Graduate Program, University of Delaware, Newark, DE, USA, [4]Department of Natural Resources Science, University of Rhode Island, Kingston, RI, USA

Key Points:

- Groundwater ammonium–N concentrations peaked following warm water temperatures, low hydraulic gradients, and high dissolved organic carbon (DOC)
- Ammonium concentrations were likely driven by seasonal changes in ammonification, nitrification, and dissimilatory nitrate reduction to ammonium (DNRA)
- Hydrologic conditions and elevated dissolved iron (Fe) concentrations likely shaped the seasonal ammonium patterns

Supporting Information:

Supporting Information may be found in the online version of this article.

Correspondence to:

M. G. Sena,
senam@udel.edu

Citation:

Sena, M. G., Peipoch, M., Joshi, B., Rahman, Md. M., Peck, E., Gold, A. J., et al. (2025). Seasonal variation and key controls of groundwater ammonium concentrations in hypoxic/anoxic riparian sediments. *Journal of Geophysical Research: Biogeosciences*, *130*, e2023JG007900. https://doi.org/10.1029/2023JG007900

Received 14 NOV 2023
Accepted 3 JAN 2025

Abstract The seasonal controls of hydrology, temperature, hypoxia, and biogeochemical conditions for groundwater ammonium–N (NH_4^+) concentrations are not well understood. Here we investigated these controls for riparian groundwaters located upstream of two milldams over a period of 4 years. Groundwater chemistry was sampled monthly while groundwater elevations, hydraulic gradients, and temperatures were recorded sub-hourly. Distinct seasonal patterns for NH_4^+ were observed which differed among the wells. For wells that displayed a strong seasonal pattern, NH_4^+ concentrations increased through the summer and peaked in October–November. These elevated concentrations were attributed to ammonification, suppression of nitrification, and/or dissimilatory nitrate reduction to ammonium (DNRA). These processes were driven by high groundwater temperatures, low hydraulic gradients (or long residence times), hypoxic/anoxic groundwater conditions, and increased availability of dissolved organic carbon as an electron donor. In contrast, NH_4^+ concentrations decreased in the riparian groundwater from January to April during cool and wet conditions. A groundwater well with elevated total dissolved iron (TdFe) concentrations had elevated NH_4^+ concentrations but displayed a muted seasonal response. In addition to hydrologic controls, we attributed this response to additional NH_4^+ contribution from Fe-driven autotrophic DNRA and/or ammonification linked to dissimilatory Fe reduction. Understanding the temporal patterns and factors controlling NH_4^+ in riparian groundwaters is important for making appropriate watershed management decisions and implementing appropriate best management practices.

Plain Language Summary Wetland or riparian soils and groundwaters depleted of oxygen can accumulate ammonium–N (NH_4^+), a toxic pollutant at high concentrations. NH_4^+ can be produced and removed via microbial processes that are influenced by seasonal factors such as: temperature, groundwater levels, dissolved oxygen, organic carbon, nitrate, and dissolved iron. In this study, we studied monthly grab samples of riparian groundwater collected upstream of milldams over a period of 4 years. We evaluated the data, identified three main seasons, and generated relationships between physical and chemical factors and NH_4^+ over time. The main findings from this study show that NH_4^+: (a) peaks in October and November when water is warm, stagnant, and high in organic carbon, (b) decreases from January – April when temperatures cooled and lowered microbial production, and (c) elevated iron groundwater concentrations can dampen these seasonal trends. Results from this study can help to improve the timing of milldam removal practices and for the management of wetlands that remove nitrogen from the terrestrial environment.

1. Introduction

Ammonium–N (NH_4^+) is an important reactive and bioavailable form of nitrogen (N) that can originate from natural and anthropogenic (fertilizer) sources in the watershed (Galloway et al., 1995; Vitousek et al., 1997). Excessive NH_4^+ concentrations in surface waters can promote eutrophication which can subsequently lead to hypoxic/anoxic conditions in aquatic ecosystems (Galloway et al., 2008; Kaplan & Bott, 1982; Vitousek et al., 1997; Yang et al., 2008). Elevated NH_4^+ concentrations can also be problematic for drinking water treatment facilities due to the formation of carcinogenic disinfection byproducts during chlorination (Zhang et al., 2022) and high NH_4^+ concentrations in surface and groundwaters can be toxic to plants and suppress root growth (Britto & Kronzucker, 2002). Thus, understanding the conditions and processes that regulate how NH_4^+

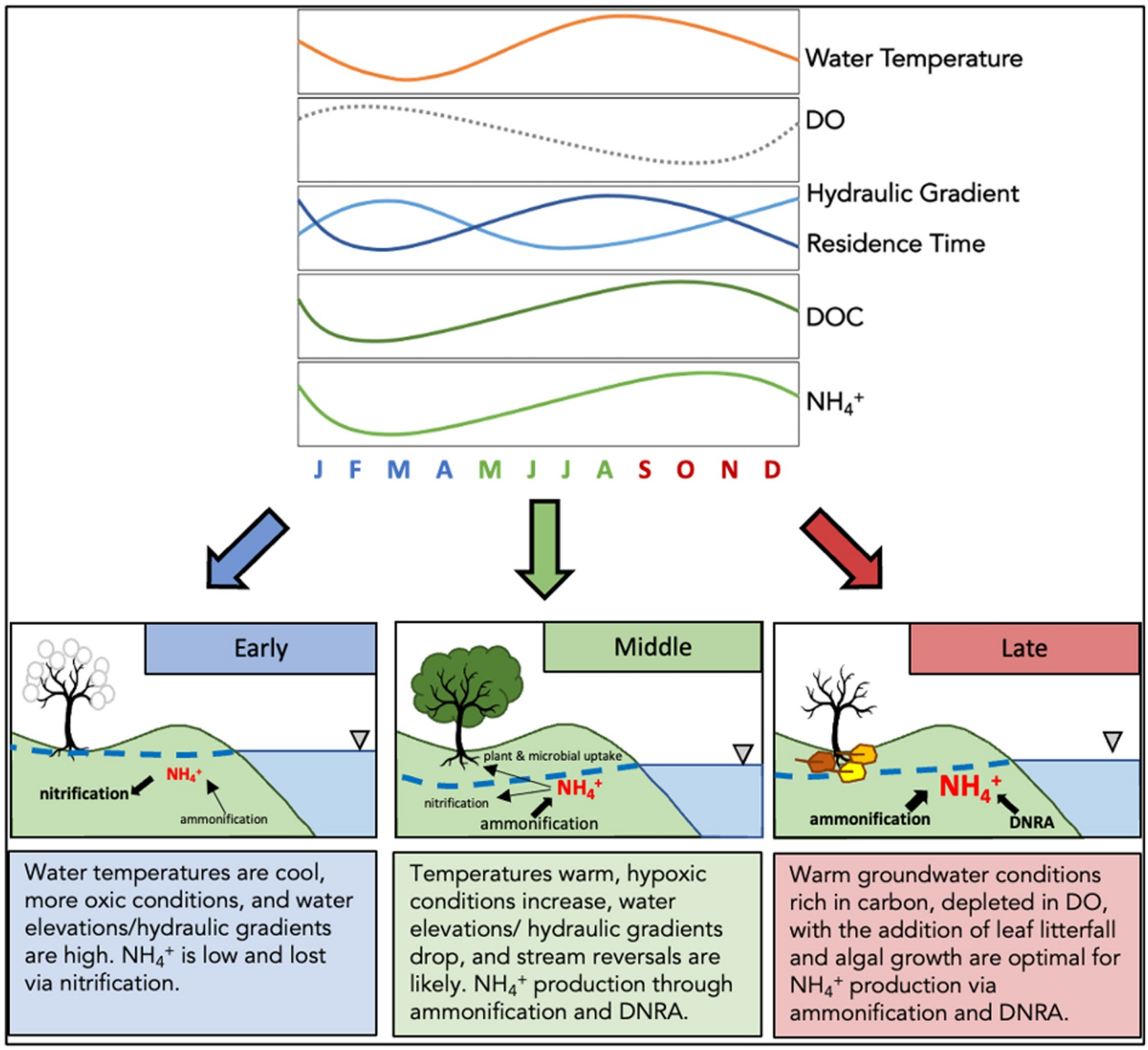

Figure 1. Conceptual diagram illustrating the seasonal changes in NH_4^+ concentrations as a function of various factors (top) - groundwater water temperature, dissolved oxygen, hydraulic gradient, residence time, and dissolved organic carbon. NH_4^+ concentrations peak in the "late" autumn period and are at their minimal during the low temperature "early" winter/spring period. Key processes involved are highlighted in the middle panel. The thickness of the arrows and the size of the text indicate the magnitude of the process and the solute pool.

concentrations vary seasonally in surface and groundwaters is important for implementing appropriate mitigation and management practices (Clune et al., 2019; Singh et al., 2021).

Key source and sink processes that could affect the production and accumulation of NH_4^+ in groundwaters and soils include: mineralization or ammonification, dissimilatory nitrate (NO_3^-) reduction to ammonium (DNRA), sorption-desorption between water and sediment exchange sites, plant and microbial uptake, annamox, and nitrification (Covatti & Grischek, 2021; Ranalli & Macalady, 2010; Zhang et al., 2020). In mineralization or ammonification, organic matter is broken down by heterotrophic microorganisms under aerobic and/or anaerobic conditions, which can result in the production of NH_4^+ (Kresic, 2007). In comparison, DNRA is carried out by obligate anaerobic microorganisms in reduced soil conditions involving the dissimilatory transformation of NO_3^- to NH_4^+ (Giblin et al., 2013; Rahman et al., 2024; Rütting et al., 2011). Annamox converts NH_4^+ to N_2 gas under anaerobic conditions, but typically occurs in sediments with low organic carbon (Reddy et al., 2022). In contrast

to DNRA, nitrification will occur in aerobic soil conditions and reduce NH_4^+ concentrations by converting NH_4^+ to NO_3^- (Zhang et al., 2020). Anoxic groundwater conditions will, however, suppress nitrification and result in accumulation of NH_4^+ in groundwaters (Yuan et al., 2023; Zhang et al., 2020).

These biotic processes could be affected by a variety of environmental conditions and factors that could shape the seasonal pattern of groundwater NH_4^+ concentrations (Liang et al., 2020; Rahman, Grace, et al., 2019; Zhao et al., 2020). Warm water and soil temperatures in summer will increase all microbial processes, including ammonification and DNRA, resulting in elevated NH_4^+ concentrations (Dai et al., 2020; Giblin et al., 2013; Yuan et al., 2023). On the other hand, warm temperatures during the growing season could decrease NH_4^+ concentrations via plant and microbial uptake (Reddy et al., 2022). Elevated surface and groundwater temperatures also lower dissolved oxygen (DO) thus fostering hypoxic/anoxic conditions for anaerobic microbial processes (Riedel, 2019). Increased groundwater residence time provides greater time for these processes to occur and could increase both source as well as sink processes affecting NH_4^+ concentrations (Covatti & Grischek, 2021). On the other hand, dry and oxygenated conditions could foster the aerobic process of nitrification and result in reduced NH_4^+ concentrations due to conversion to NO_3^- (Rahman, Grace, et al., 2019). Increased availability of electron donors such as DOC and iron (Fe) increase DNRA rates (Pandey et al., 2020; Rütting et al., 2011). Similarly, soils with high Fe concentrations have been reported to have higher ammonification rates as Fe^{3+} in Fe oxides serves as an electron acceptor for the oxidation of organic matter, the reduction to Fe^{2+}, and ultimately the production of NH_4^+ (Emsens et al., 2016; Pan et al., 2016; Sahrawat, 2004). The eventual expression of NH_4^+ in groundwaters is dictated by a complex interaction of all of these factors and conditions.

Inamdar et al. (2022) reported elevated concentrations of NH_4^+ (as high as 30 mg N/L) for stagnant and hypoxic/anoxic riparian groundwaters upstream of milldams in the mid-Atlantic region of the United States (US). Anaerobic mineralization, suppression of nitrification, and DNRA were identified as the potential mechanisms contributing to the elevated dissolved NH_4^+ concentrations (Inamdar et al., 2022; Lewis et al., 2021; Peck et al., 2022). Recent work by Rahman et al. (2024) has confirmed that DNRA is indeed occurring at the sites and elevated DOC and Fe concentrations were likely driving the heterotrophic and autotrophic forms of the process, respectively. While Inamdar et al. (2022) highlighted the spatial variability of these factors for NH_4^+, their temporal/seasonal influence on groundwater NH_4^+ concentrations were not explored and is unknown.

The goal of this study was to extend the work of Inamdar et al. (2022) by investigating the temporal/seasonal variation in groundwater NH_4^+ concentrations and to identify the key drivers responsible for these changes. Key questions addressed were: (a) How do riparian groundwater NH_4^+ concentrations change over time? (b) What are the key processes and factors driving the temporal patterns in NH_4^+? and (c) What are the broader implications of the seasonal NH_4^+ variability for watershed management? This work used the same riparian sites studied by Inamdar et al. (2022) but focused on selected groundwater wells with the highest NH_4^+concentrations and an extended dataset with a total of 4 years (November 2019–2023) of data. We hypothesized that the seasonal patterns of groundwater NH_4^+ would be primarily driven by groundwater temperatures, hypoxic/anoxic conditions, and elevated groundwater levels and residence time. Secondarily, we also hypothesized availability of electron donors and acceptors (DOC, Fe and NO_3^-) could also affect the production of NH_4^+, with ammonification followed by DNRA and the suppression of nitrification as potential processes shaping this seasonality.

2. Site Description and Methods

2.1. Site Description

The two riparian sites used in this study were both located in unglaciated watersheds within the Piedmont physiographic region of the mid-Atlantic US that were immediately upstream of milldams (Figure 2). The Roller Milldam (2.4 m tall; 30 m wide) is located on Chiques Creek near Manheim, PA (coordinates: 40.108,306, −76.443,111) and was built ∼ 1,730. The area is mostly agricultural (54%) and forested (26%) (Homer & Barnes, 2012). The parent material is Piedmont sediment and the soils in the riparian zones are classified as Hagerstown silt loams (HaB) and silty clay loams (HbD) (Soil Survey, 2021). The mean annual precipitation is 104 cm and mean annual temperature is 15.5°C (NOAA, 2021).

The Cooch Milldam (4 m tall; 40 m wide) is located on the Christina River in Newark, DE (coordinates: 39.645,556, −75.742,500). The area is mostly developed (47%) and forested (30%) land (Homer & Barnes, 2012). The parent material is Piedmont sediment primarily composed of Iron Hill gabbro and soils classified as Hatboro-

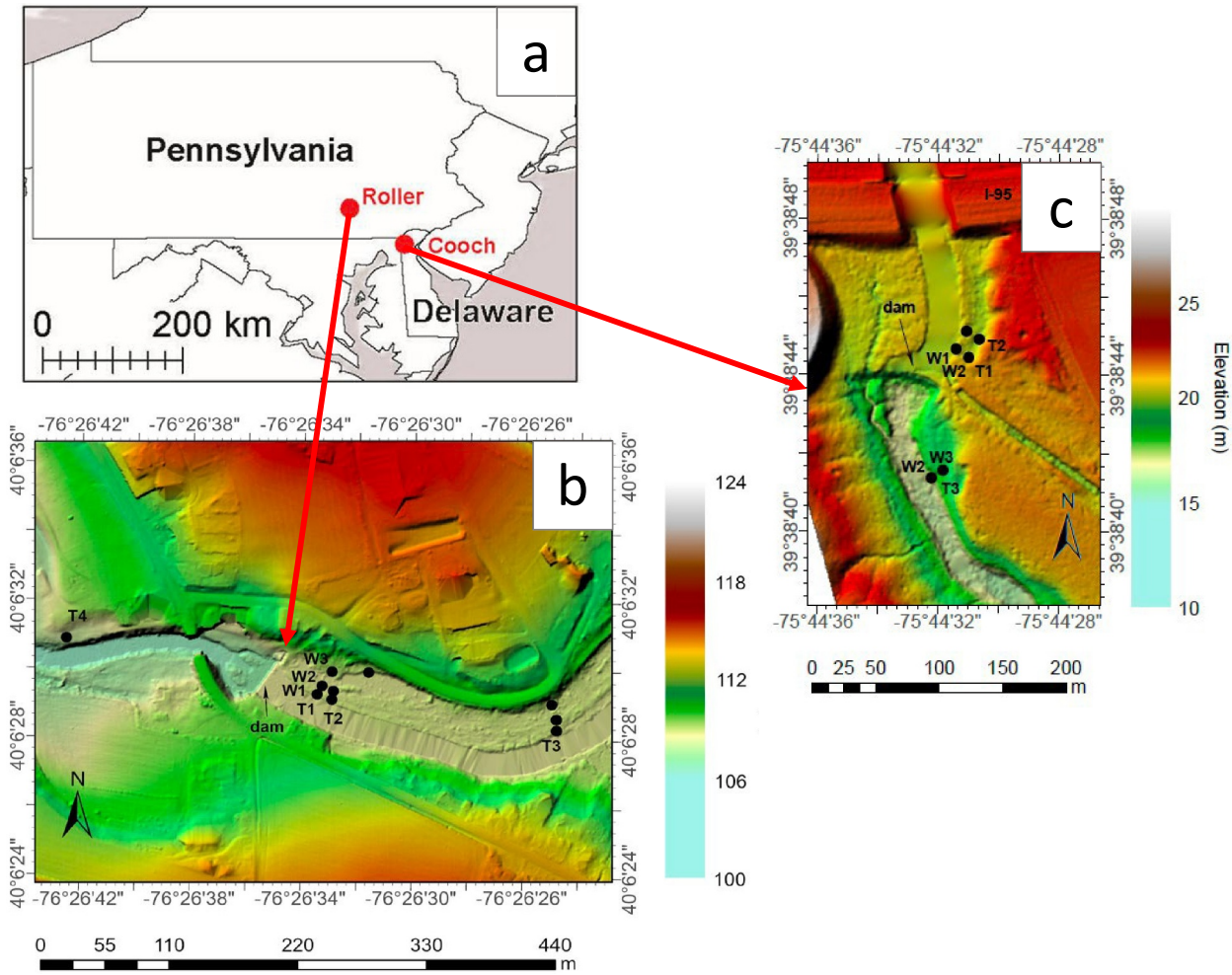

Figure 2. Map showing the location of the Roller and Cooch sites (a.) and LIDAR images of both the Roller (b.) and Cooch (c.) milldams and the sampling transects that were used for this study (Inamdar et al., 2022; Sherman et al., 2022).

Codorus (Hw; poorly drained), Keyport (KpB; moderately drained), and Mattapex (MtaB) silt loams (Soil Survey, 2021). Mean annual precipitation is 114 cm and temperature is 12.2°C (NOAA, 2021).

2.2. Hydrologic Monitoring and Water Sampling

Hydrologic monitoring and water sampling procedures were previously described in detail by Inamdar et al. (2022) and Sherman et al. (2022). Riparian groundwater wells were installed at the near-stream "berm" location (well W1), swale location (well W2), and the riparian upland edge (well W3). Wells were constructed of PVC and were ~3–4 m depth at the berm location and ~1–1.5 m at the swale and upland edge locations (Figure 2). These groundwater wells were capped at the top and screened below 0.3 m below the soil surface to prevent surface and groundwater mixing during precipitation events. Since the NH_4^+ concentrations were highest in the near-stream wells (W1) (Inamdar et al., 2022), only data from these wells were used in this study. One transect (T1) was used at the Roller site and two transects (T1 - T2) were used at the Cooch site. Groundwater samples were available monthly from November 2019–2023 (4-year time period). For the same time period, groundwater elevation and temperature data were available at a 30 min interval for the wells and were recorded using a pressure transducer (HOBO U20 L; Sherman et al., 2022). Groundwater elevations (m), depth to groundwater from soil surface (DTW; m), and hydraulic gradients (m/m) from the wells to the stream were previously computed by Sherman et al. (2022) and were used here to characterize the hydrologic conditions. In addition, air temperature data downloaded from the Delaware Environmental Observing System at the Newark, DE Ag–Farm for Cooch

and National Weather Service at the Lancaster, PA Airport for Roller were also included to assess the lag in groundwater temperature versus the air values.

2.3. Dissolved Oxygen

Using discrete point measurements, Inamdar et al. (2022) previously showed that riparian groundwater wells were hypoxic/anoxic year round. Since September 2022, however, we installed high-frequency (every 30 min) DO sensors/loggers (Onset HOBO U26) in the two creeks upstream of the dams and the berm well at Roller (RMT1W1). The well DO was persistently anoxic (flat line at zero) and thus is not included but DO data from the streams (September 2022–August 2024) is included to highlight the seasonal DO variation and periods of lowest DO in the milldam-affected stream-riparian system.

2.4. Water Chemistry Analysis

Groundwater and stream water samples were collected in acid–washed 250 mL Nalgene HDPE plastic wide mouth bottles, filtered using Sterlitech Grade F (0.7 μ m) filters, and acidified to a pH < 2 using reagent grade HCl. NH_4^+ and NO_3^- were measured colorimetrically using a Bran and Luebbe AutoAnalyzer 3 (Bran and Luebbe, Buffalo Grove, IL). Total organic carbon and total nitrogen were measured by direct combustion using an Elementar Vario-Cube TOC Analyzer (Elementar Americas, Mt. Holly, NJ). Dissolved TdFe and Na^+ were analyzed by inductively coupled plasma optical emission spectroscopy using an iCAP 7,600 Duo View ICP-OES (Thermo Scientific, Madison, WI).

2.5. Data Analysis

Monthly water chemistry data were averaged over the 4-year period (November 2019–2023) to generate an average monthly temporal trend. Similarly, DTW, hydraulic gradients, and temperature, which were measured at 30 min intervals, were averaged to monthly values to allow for direct comparison with measured groundwater chemistry data. The data were analyzed through simple and multiple linear regression and Spearman correlation coefficient analyses in *R* Studio (R Core Team) and plotted using the "ggplot2" package. Principal component analysis (PCA) was performed in JMP version 17.0.0. Results from PCA were used to group the groundwater data based on physical (temperature and DTW) and chemical (NH_4^+, NO_3^-, DOC, TdFe, and Na^+ concentrations) characteristics and to delineate three-time blocks or "seasons" based on groundwater chemistry patterns within the year: "Early" from January–April (blue color in Figures 3 and 4); "Middle" from May–August (green color in Figures 3 and 4);, and "Late" from September–December (red colors in Figures 3 and 4). Statistical significance and slight statistical significance were assessed at 0.05 and 0.05–0.10 confidence levels, respectively.

3. Results

3.1. Temporal Changes in Riparian Groundwater Physical and Chemical Properties

Mean groundwater temperatures over the 4-year study period for the Roller and Cooch berm wells were similar with warmest values from September – October (Late period) and coolest in March (Early period, Figures 3a–3c). In contrast, air temperatures (Figure S1 in Supporting Information S1) were warmest in July–August and coolest in January–February; indicating a 1–2 month lag in groundwater temperatures behind the atmospheric values. DTW for the same period indicated that groundwater was closest to the soil surface from March – May and fell to the lowest annual point below the soil surface during August (Figures 3d–3f). Based on DTW, CMT1W1 was the driest and CMT2W1 the wettest, with RMT1W1 having intermediate values (Figures 3d–3f). This trend is also clearly supported by the cumulative 4-year DTW curve indicating the % time at various depths (Figure S2 in Supporting Information S1). We also observed greater variability in DTW for the RMT1W1 and CMT1W1 wells versus the CM2T1W1 well. Similarly, groundwater hydraulic gradients (Figures 3g–3i) from the wells to the streams were at their minimum from June – August and highest in March – April at the Cooch site but were elevated from December–April at the Roller berm well (RMT1W1). The Cooch berm wells (Figures 3h and 3i) also displayed negative hydraulic gradients indicating that the groundwater flow was orthogonal from the stream to the well, with the greatest reversals (negative gradients) occurring between June – August. Periods of low hydraulic gradients indicate greater groundwater residence time during those periods. Again, similar to the muted variation in DTW, CMT2W1 displayed the lowest changes in hydraulic gradients among the three wells.

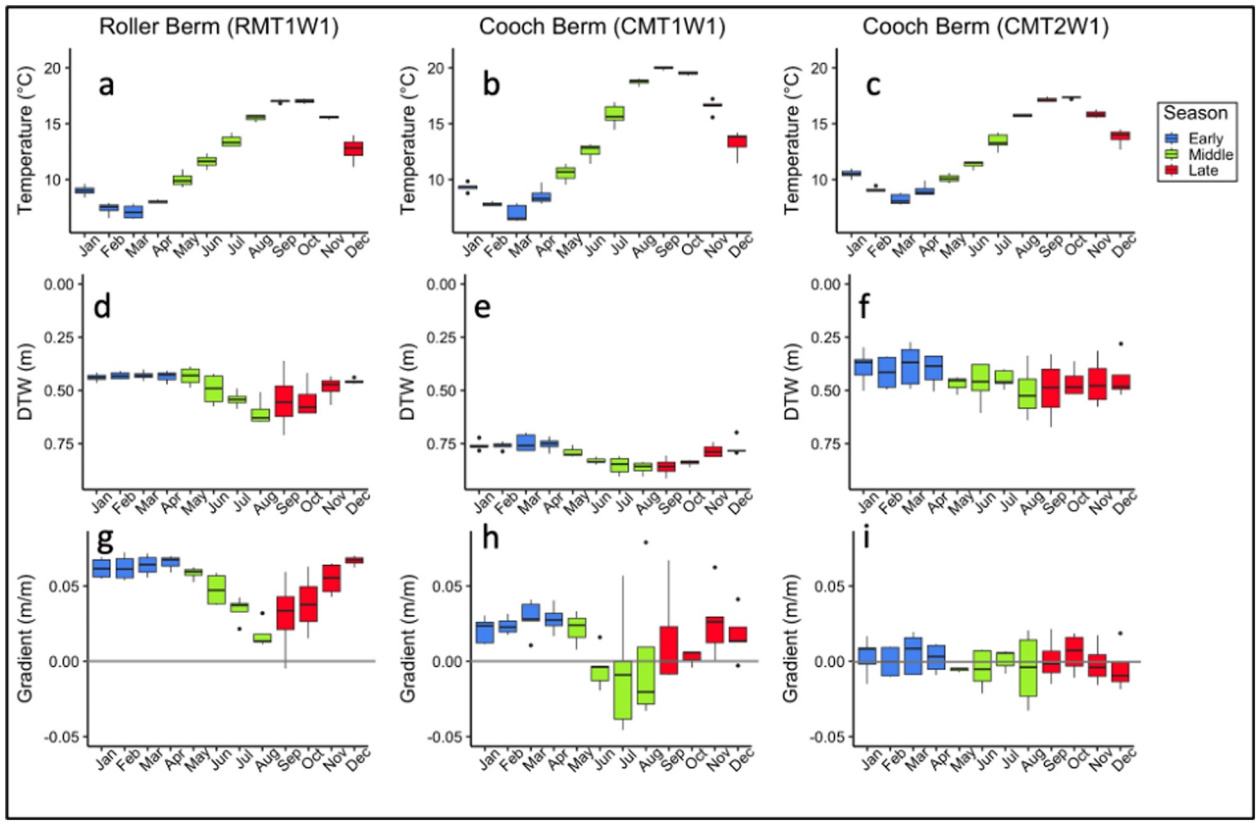

Figure 3. Mean monthly riparian groundwater values (averaged over the 4 year study period) for temperature (°C) (a–c), depth to water (m) (d–f), and hydraulic gradient (m/m). Positive hydraulic gradients indicate groundwater flow from riparian to stream and vice versa. Data were grouped into three "seasons"–blue–Early (January–April); green–Middle (May–August); and Late year (September–December).

NH_4^+ concentrations for the RMT1W1 and CMT1W1 wells declined early in the year from January to April (Figures 4a and 4b) during the same time when groundwater temperatures cooled and water levels and hydraulic gradients were elevated (Figure 3). In contrast, NH_4^+ concentrations increased at these wells in September and peaked in November following warmest groundwater temperatures in September and October (Figures 4a and 4b). Although NH_4^+ concentrations for well CMT2W1 (Figure 4c) also declined from January to April and were greater in the summer and autumn, they did not match the pronounced seasonal variations of the other two wells. We should also note that the magnitude of NH_4^+ concentrations differed among the three wells–highest at CMT2W1, intermediate for RMT1W1, and lowest for the CMT1W1 well (Figures 4a–4c). Although NO_3^- was consistently <1.5 mg N/L throughout the study period for all three wells, values for Roller well (RMT1W1) were greater than those for the Cooch wells. NO_3^- concentrations at RMT1W1 increased from January – April while NH_4^+ concentrations were declining. Conversely, NO_3^- concentrations declined from May to November while NH_4^+ concentrations were increasing at RMT1W1 (Figure 4d). This trend was not observed at the Cooch wells, where NO_3^- concentrations fluctuated little over time (Figures 4e and 4f). Dissolved organic carbon concentrations increased throughout the year at RMT1W1 and CMT2W1, where concentrations were lowest in February, 2–3 months before the lowest mean in NH_4^+ concentrations, followed by an increase until November (Figures 4g and 4i). Conversely at CMT1W1, concentrations of DOC increased from January – April, dropped from May – June, and were consistently lower from the months of July – December (Figure 4h). Trends with TdFe over time/seasons were not clear, but concentrations at the CMT2W1 well were higher and more variable (Figure 4l) than either the RMT1W1 or CMT1W1 wells (Figures 4j and 4k). Similar to TdFe, the magnitude and temporal changes in Na^+ concentrations varied by well. At RMT1W1, Na^+ concentrations were consistently low (<50 mg/L) and varied little over time (Figure 4m). However, at CMT1W1, Na^+ concentrations were elevated with a seasonal trend of high values in the Early period, lowest in the Middle period, and then an increase in the Later period (Figure 4n). Surprisingly, this trend was not observed at CMT2W1, where Na^+ concentrations were highest in

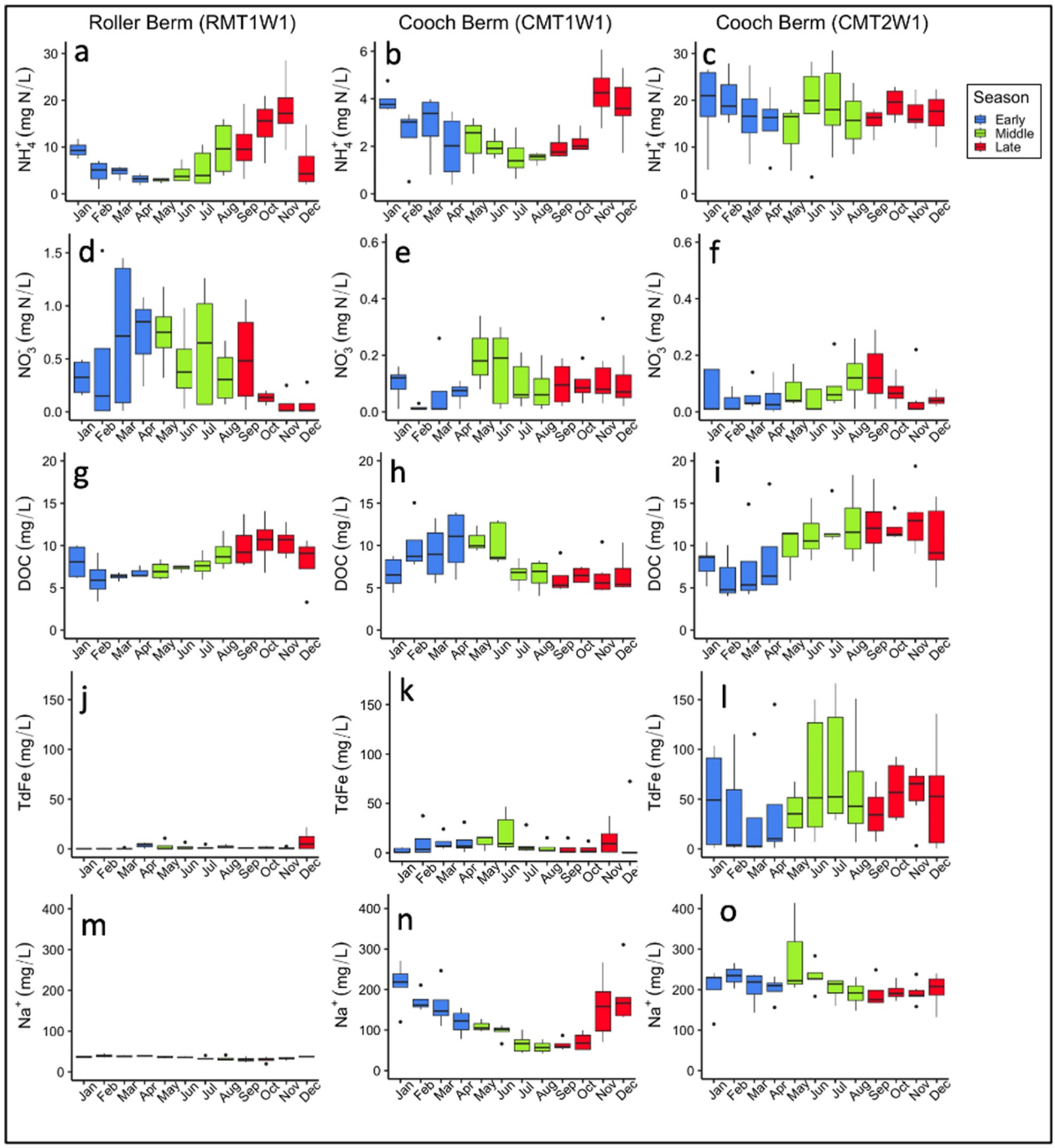

Figure 4. Mean monthly concentrations (mg/L) over the 4-year study period for NH_4^+ (a–c), NO_3^- (d–f), dissolved organic carbon (g–i), and TdFe (j–l) for the Roller berm (RMT1W1, left), Cooch berm at Transect 1 (CMT1W1, middle) and Cooch berm at Transect 2 (CMT2W1, right) wells. Data were grouped into three "seasons"–blue–Early (January – April); green–Middle (May – August); and red–Late (September – December) year.

May but consistent throughout the rest of the year (Figure 4o) (as noted in Inamdar et al. (2022), well CMT2W1 was closer to the upstream storm drain that discharged road salt runoff into this riparian zone).

3.2. Seasonal Trends From Principal Component Analysis

Principal component analysis results for the RMT1W1 and CMT1W1 wells show a clear seasonal separation of the monthly data driven by NH_4^+, NO_3^-, DOC, TdFe, and Na^+ concentrations and physical DTW and

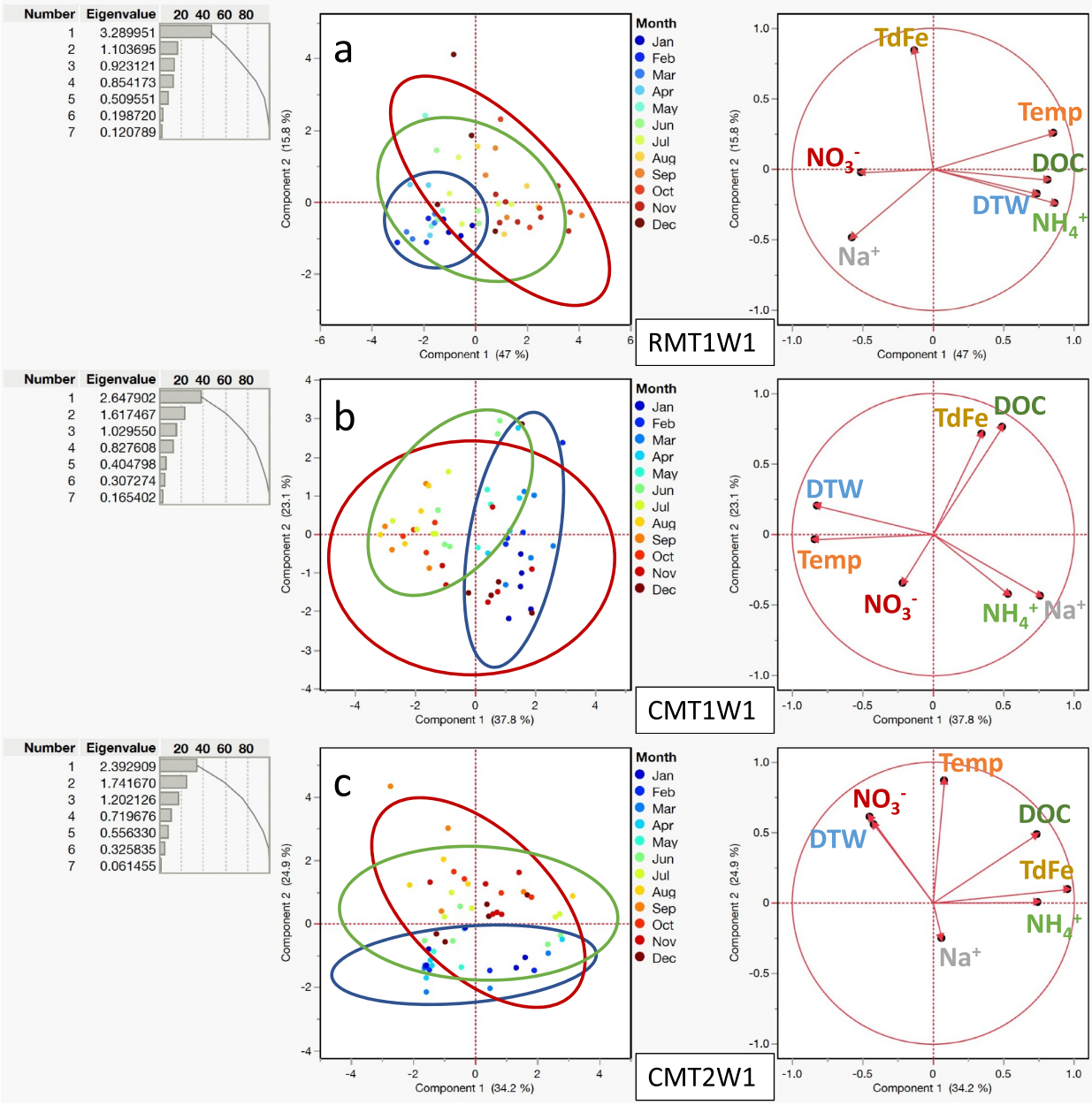

Figure 5. Principal component analysis score (left) and loading (right) plots for the (a) Roller berm (RMT1W1), (b) Cooch berm Transect 1 (CMT1W1), and (c) Cooch berm Transect 2 (CMT2W1) wells.

temperature parameters (Figures 5a and 5b). Here, three main seasons emerged: winter to early spring (January – April), late spring to summer (May–August) and fall to early winter (September–December). However, there were some differences between the RMT1W1 and CMT1W1 wells that should be noted. For example, at RMT1W1, NH_4^+ and DOC concentrations tend to increase with temperature and DTW during the late summer/fall season while Na^+ and NO_3^- concentrations tend to increase during the winter/early spring season (Figure 5a). TdFe concentrations did not follow a clear seasonal trend in the PCA at RMT1W1 (Figure 5a). NH_4^+ concentrations were highest later in the year at CMT1W1, similar to RMT1W1, but increased with Na^+ more than DOC (Figure 5b).

The seasonal separation was, however, not as clear at CMT2W1 as it was for the other two wells (Figure 5c). There was still a general clustering for samples between the months of September – December and January –

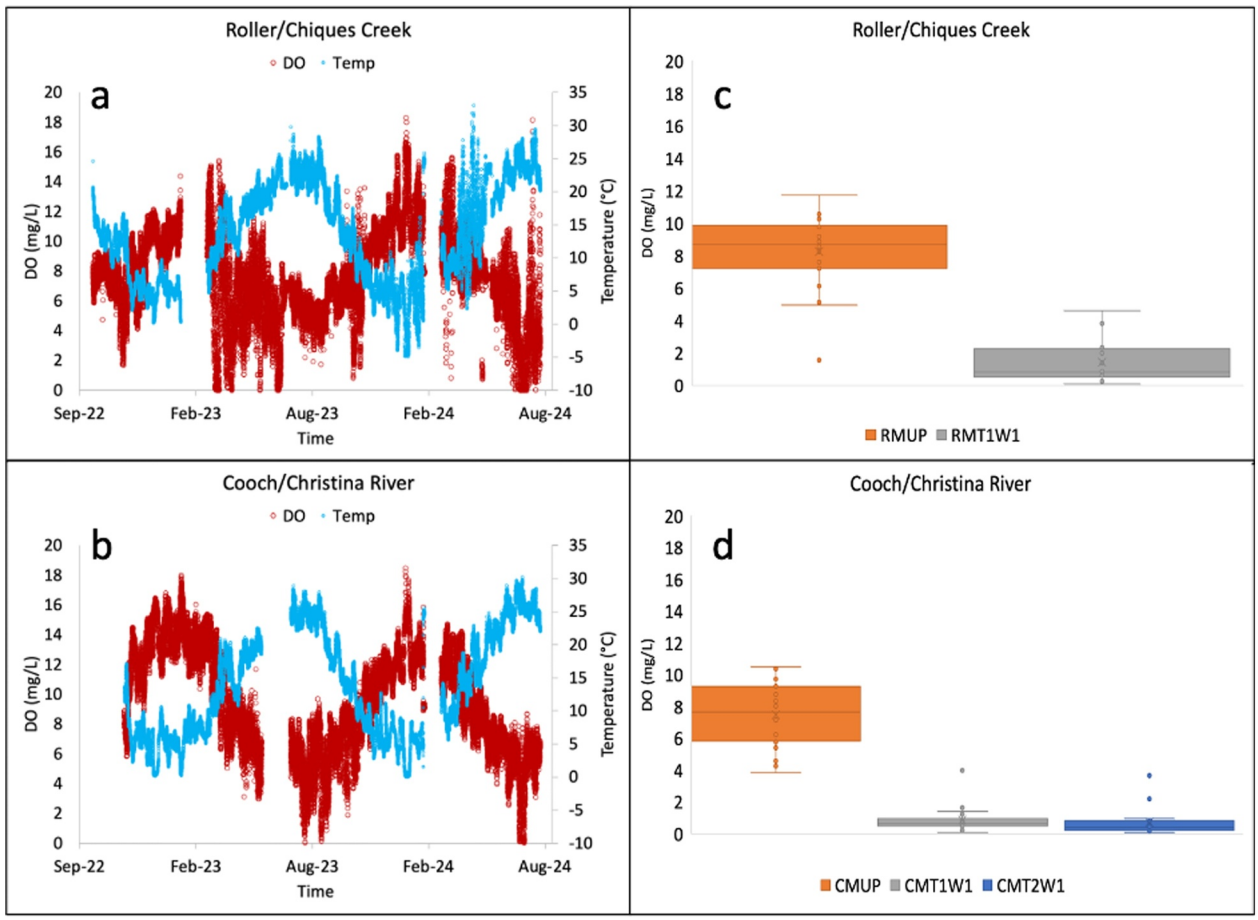

Figure 6. Dissolved oxygen (DO) - red - versus temperature - blue - relationships at the (a). Chiques Creek (Roller) and (b). Christina River (Cooch) from September 2022 – August 2024 and (c). boxplots of DO at Chiques Creek (orange) and RMT1W1 (gray) and (d). boxplots of DO at Christina River (orange), CMT1W1 (gray), and CMT2W1 (blue) from November 2019 - July 2022.

April, but the middle time period between May – August was not as well-defined. At this well, NH_4^+ concentrations generally increased with DOC and TdFe (Figure 5c), which contrasts with the trends at the RMT1W1 and CMT1W1 wells where TdFe concentrations moved in opposing directions to NH_4^+ (Figures 5a and 5b).

3.3. Seasonal Dissolved Oxygen Patterns for Streams Upstream of the Dam

High-frequency (30 min) stream water DO upstream of the dams for both sites displayed a strong seasonal trend. Despite slight differences between the Chiques Creek and Christina River, the DO values were generally at their highest (~18 mg/L) during low temperature winter (January/February) conditions and lowest (~0 mg/L) in late summer (July–September) corresponding with high stream water temperatures (Figures 6a and 6b). Chiques Creek also displayed occasional drops in early spring of 2023 likely corresponding to high sediment and nutrient loads associated with storms. In contrast, monthly DO data for the groundwater wells (presented earlier in Inamdar et al., 2022 and reproduced here as box plots in Figures 6c and 6d) revealed persistently hypoxic/anoxic conditions (high frequency data was not available for all wells). Taken together, the stream-riparian system above the dam was most hypoxic/anoxic in late summer (July–September) and most oxic in winter (January–February).

3.4. Spearman Correlations

NH_4^+ concentrations at RMT1W1 were positively correlated with DOC, temperature, and DTW for the full year ($r = 0.72$, 0.49, and 0.42, respectively) while NO_3^- and Na^+ were negatively correlated ($r = -0.47$ and -0.39, respectively) (Table 1). The positive relationship with DOC strengthened later in the year, increasing from $r = 0.54$ Early to 0.88 Late. Overall, the correlations were highest between May – August, where NO_3^-, hydraulic

Table 1
Spearman Correlation Coefficients and Significance Levels Between NH_4^+ and the Listed Variables

RMT1W1	Time of year			
Variable	All	Early	Middle	Late
DTW	0.42	0.11	0.84	0.53
Gradient	−0.26	−0.13	−0.64	−0.41
Temperature	0.49	0.44	0.57	0.31
DOC	0.72	0.54	0.60	0.88
TdFe	−0.10	−0.24	−0.09	−0.19
NO3-	−0.47	−0.20	−0.88	0.05
Na+	−0.39	−0.50	−0.22	−0.19
CMT1W1				
Variable	All	Early	Middle	Late
DTW	−0.36	0.13	−0.10	−0.57
Gradient	0.08	−0.39	−0.16	−0.01
Temperature	−0.20	0.32	−0.33	−0.58
DOC	−0.05	−0.06	0.53	−0.09
TdFe	−0.10	−0.11	0.71	−0.23
NO3-	−0.15	−0.05	−0.34	0.09
Na+	0.52	0.08	0.42	0.78
CMT2W1				
Variable	All	Early	Middle	Late
DTW	−0.15	0.06	−0.50	0.12
Gradient	0.18	−0.11	0.55	−0.16
Temperature	−0.03	0.23	−0.02	−0.15
DOC	0.24	0.51	0.34	−0.02
TdFe	0.72	0.91	0.75	0.53
NO3-	−0.20	0.08	−0.50	−0.02
Na+	0.29	0.77	−0.39	0.45

Note. Dark blue (+) and dark orange (−) = p-value <0.05; light blue (+) and light orange (−) = p-value 0.05–0.10. "all" is the correlation for the full time period while "Early" is from January – April, "Middle" from May – August, and "Late" from September – December

gradient, and temperature were only statistically significant during this time ($r = -0.88$, -0.64, and 0.57, respectively).

The correlation values for CMT1W1 over the total time period were lower than that of RMT1W1, where only Na^+ and DTW were significantly correlated ($r = 0.52$ and -0.36, respectively). We did not observe any significant relationships early in the year at this well. Similar to RMT1W1, though, relationships strengthened in the middle of the year, where correlations for TdFe ($r = 0.71$) and DOC ($r = 0.53$) increased dramatically from earlier in the year. The highest correlations late in the year at this well were Na^+ ($r = 0.78$), temperature ($r = -0.58$), and DTW ($r = -0.57$) (Table 1).

The strongest correlations with NH_4^+ at CMT2W1 were for TdFe ($r = 0.72$) and Na^+ ($r = 0.29$), where the relationship between NH_4^+ and TdFe was significant for all three time periods while Na^+ was only significant early and slightly significant late in the year (Table 1). Correlations between NH_4^+ and DOC declined throughout the year ($r = 0.51$ Early, 0.34 Middle, and -0.02 Late), a trend opposite to what we observed at RMT1W1. Similar to RMT1W1, hydraulic gradient ($r = 0.55$) and DTW ($r = -0.50$) showed the highest correlations from May – August, except the direction of the relationship was reversed. Also similar to RMT1W1, the correlations with NO_3^- were highest from May – August ($r = -0.50$) (Table 1).

4. Discussion

This study revealed distinct temporal/seasonal patterns in groundwater NH_4^+ concentrations for the Roller and Cooch wells RMT1W1 and CMT1W1, respectively, which aligned with our hypothesized patterns in Figure 1. Seasonal NH_4^+ patterns for the wettest and Fe-rich Cooch well CMT2W1, were however, muted suggesting differences in hydrologic and biogeochemical controls for this well We elaborate on these seasonal differences and the key mechanisms and factors that may be driving the seasonal patterns.

4.1. Strong Temporal Variation in NH_4^+ Concentrations and Key Drivers

Both the RMT1W1 and CMT1W1 wells displayed declining trends in NH_4^+ concentrations early in the year (January – April) and an increasing trend from August with a peak in values in November (Figures 3a and 3b). These changes in concentrations can be explained by three potential mechanisms: (a) warmer water temperatures and lowered hydraulic gradients increase microbial activity rates and residence time that depletes DO and produces NH_4^+ via ammonification and/or DNRA; (b) seasonal changes in electron donor to acceptor (DOC:NO_3^-) ratios, where DOC acts as an electron donor and can promote DNRA at higher concentrations; and (c) algal die-off and decay and leaf litter-fall in the streams can further deplete DO, creating ideal conditions for NH_4^+ production through ammonification and DNRA. These reasons are discussed further below and are highlighted in Figure 1.

4.1.1. Controls of Groundwater Temperature and Hydrology

Warmer water temperatures, as observed in September – October (Figure 3), can decrease DO concentrations in the groundwater by promoting increased rates of microbial respiration (Farnsworth & Hering, 2011; Harvey et al., 2011; Kadlec & Reddy, 2001). Additionally, low groundwater elevations and hydraulic gradients, as observed in August (Figure 3), can increase residence time while high gradients from January – April can decrease the groundwater residence time. Higher residence times provide more time for microbial respiration to occur, which can further decrease DO and create more anoxic conditions. We hypothesize that these conditions facilitated NH_4^+ production and accumulation in riparian soils (conceptual model in Figure 1) during August–

October through the process of ammonification (Dai et al., 2020) and/or DNRA (Pandey et al., 2020; Rubol et al., 2013; Rütting et al., 2011). The simultaneous decrease in NO_3^- concentrations during this time would also support the DNRA conversion to NH_4^+. There was, however, a 1–2 month lag between peak groundwater temperatures and peak NH_4^+ concentrations (Figures 3 and 4). This delay could be associated with the lag in biogeochemical processes as well as the wetting-up duration of the soil profile from September – November (Figures 3d–3f) after its minima in August. The wetting-up of the soils during September–November likely mobilized the NH_4^+ from the soils into the groundwaters.

After the peak in November, groundwater NH_4^+ concentrations declined through the winter months concomitant with decreasing groundwater temperatures along with increasing groundwater levels and hydraulic gradients (Figures 3 and 4). Decreasing winter temperatures and increasing hydraulic gradients likely reduced NH_4^+ production and may have also slightly oxygenated the groundwaters leading to the conversion of NH_4^+ to NO_3^- via nitrification, which was eventually lost via denitrification. Groundwater N concentrations in spring (April–June) remained low and were likely influenced by increasing riparian plant and microbial uptake following the winter dormant season.

Other studies have also reported seasonal changes of NH_4^+ with typically warmer conditions increasing NH_4^+ concentrations through processes of ammonification and DNRA (An & Gardner, 2002; Chen et al., 2023; Han et al., 2023; Wang et al., 2020; Yuan et al., 2023). Han et al. (2023) attributed the elevated groundwater NH_4^+ concentrations along a sandy to clay landscape gradient in Mongolia primarily to mineralization/ammonification. Similarly, Chen et al. (2023) attributed changing NH_4^+ concentrations to both ammonification and DNRA in riverbanks in China and found that the concentrations were highest in the wet and warm season. In comparison, a study by Liang et al., 2020 found that stream NH_4^+ concentrations were higher from the dry months of January – March than the wet months of May – September due to increased fertilizer inputs and NO_3^- being converted to NH_4^+ through DNRA in the deeper groundwater supply.

4.1.2. Influence of Electron Donors and Acceptors

Ratios of DOC and NO_3^- supplies change seasonally and play an important role in the production of NH_4^+. For DNRA, DOC acts as an electron donor while NO_3^- acts as an electron acceptor, and since eight electrons need to be transferred to reduce NO_3^- to NH_4^+, DNRA rates tend to increase with soil C:N (Tiedje, 1988) and water DOC:NO_3^- ratios (Wei et al., 2022). Our recent work at these sites (Rahman et al., 2024) has confirmed that DNRA rates were higher for elevated DOC:NO_3^- ratios suggesting stimulation of heterotrophic DNRA. Here, we observed a strong seasonal pattern for groundwater DOC, especially for wells RMT1W1 and CMT2W1 (Figure 4), with concentrations increasing through June – October and peaking later in the year. This DOC pattern and elevated DOC:NO_3^- ratios later in the year could support the production of NH_4^+ via DNRA.

We should note, however, that the NH_4^+ concentrations in the wells were fairly elevated and much greater than the corresponding groundwater NO_3^- concentrations. This was particularly so for the Cooch wells. This disparity suggests that DNRA was likely not the dominant process and that ammonification was likely the key process for NH_4^+ production at these sites. The work of Rahman et al. (2024) also indicated that while DNRA was occurring, it alone could not explain the elevated NH_4^+ concentrations at these sites. As alluded to by Inamdar et al. (2022), buried organic matter and precolonial hydric layers could have been the potential source for ammonification.

4.1.3. Effects of In-Stream Conditions and Groundwater Connection

While the stream water NH_4^+ concentrations were very low year-round (Inamdar et al., 2022) and likely did not affect the groundwater NH_4^+ concentrations, the DO conditions in the stream (e.g., Figure 6), particularly in the ponded reach immediately upstream of the dam and in the proximity of the groundwater wells, could be a factor (e.g., Farnsworth & Hering, 2011). Stream water DO was generally highest during the cold months of January–March (Figure 6). In contrast, stream water DO values were at their lowest during July–September because of the elevated stream water temperatures and the quiescent and low flow hydrologic conditions during this period (Hripto et al., 2022). Additionally, DO consumption from decomposing stream algae and leaf litter that typically accumulates above the dam over this period could contribute to the depletion of DO (Figure S3 in Supporting Information S1). These stream conditions could have also influenced the adjacent riparian groundwaters, particularly wells RMT1W1 and CMT1W1, that revealed the largest seasonal variations in hydraulic gradients (Figures 3g and 3h). The reversals of gradients and the flow of low DO, C-rich stream waters into the riparian

zone could have likely further enhanced the conditions for NH_4^+ production and accumulation along the stream-riparian interface.

4.2. Damped Seasonal Response of NH_4^+ Concentrations for Well CMT2W1 and Potential Drivers

Compared to wells RMT1W1 and CMT1W1, the seasonal groundwater NH_4^+ concentrations for well CMT2W1 were muted (Figure 3c). We hypothesize that this could have been due to the lack of seasonal variation in DTW and hydraulic gradients for this well or the effect of year-round elevated TdFe concentrations. Persistently wet conditions with low hydraulic gradients, which result in hypoxic/anoxic conditions and long residence times, are ideal for production and retention of N in NH_4^+ form.

This well had persistently elevated TdFe concentrations (mean of 53.16 mg/L) versus the RMT1W1 (1.91 mg/L) and CMT1W1 (9.85 mg/L) wells (Table S1 in Supporting Information S1 and Inamdar et al., 2022). Although both the Roller and Cooch sites are in the Piedmont physiological region, the source bedrock is different. The Roller (Chiques watershed) is composed of calcium-rich dolomite and limestone while the Cooch (Christina watershed) is composed of Iron Hill gabbro, a deeply weathered rock rich in Fe oxides (Ramsey, 2005). In addition, our visual observations of exposed stream banks in this Iron Hill gabbro watershed and region indicate concentrated deposits of oxidized Fe (Supplementary Figure S4 in Supporting Information S1). These locations represent groundwater seeps carrying Fe-rich groundwaters have been exposed to oxygen resulting in oxidation and deposition to ferric oxides. We speculate that the CMT2W1 well likely intersected such a Fe-rich groundwater seep and which is contributing to the persistently elevated TdFe concentrations measured in the well.

Most (>90%) of the TdFe recorded in the groundwater wells at our study sites is in Fe^{2+} form (Rahman et al., 2024). Similar to DOC, Fe^{2+} is an important electron donor and can contribute to NH_4^+ production via autotrophic DNRA (Pandey et al., 2020; Rahman, Roberts, et al., 2019, 2024; Robertson et al., 2016; Robertson & Thamdrup, 2017). In addition, in reducing soils with elevated levels of Fe oxides, Fe^{3+} can serve as an electron acceptor and stimulate organic matter mineralization (also referred to as dissimilatory Fe reduction) with subsequent release of NH_4^+ into groundwaters (Emsens et al., 2016; Pan et al., 2016; Sahrawat, 2004). Research has also suggested that specific mineral forms (e.g., poorly crystalline Fe oxides such as ferrihydrite) at specific concentrations are key in driving the process (Mark Jensen et al., 2003; Thamdrup, 2000).

Regression relationships between groundwater NH_4^+ and TdFe concentrations for the wells revealed important differences (Figure 7 and Spearman Correlations in Table 1). For well CMT2W1, groundwater NH_4^+ concentrations increased sharply, particularly for TdFe concentrations exceeding 40 mg/L (Figure 7b). This same pattern was not replicated for wells RMT1W1 and CMT1W1 where TdFe concentrations were below 40 mg/L (Figures 7a–7c and 7d). We speculate that the Fe-rich soils and elevated TdFe concentrations for the CMT2W1 well likely stimulated organic matter mineralization and/or autotrophic DNRA and contributed to the elevated NH_4^+ at this well. The persistently elevated Fe concentrations, in combination with persistently high groundwater elevations and reducing conditions, likely provided a continuous supply of Fe for year-round production of NH_4^+ which could have played a role in damping out the effects of other seasonal drivers. However, future research is needed to explicitly test this speculation and investigate reasons and mechanisms behind the strong increase in NH_4^+ concentrations beyond the TdFe concentration of 40 mg/L.

5. Conclusions

This study revealed important seasonal patterns and key controls for NH_4^+ concentrations in reducing riparian groundwaters upstream of milldams. We found that elevated groundwater temperatures and low hydraulic gradients (or increased residence time) in late summer/early autumn promoted hypoxic/anoxic conditions in riparian sediments that increased the availability of electron donors stimulating the production and accumulation of NH_4^+. Ammonification, suppression of nitrification, and/or heterotrophic DNRA were proposed as the key mechanisms driving this change. These observations suggest that there could be a "sensitive" seasonal time window in late summer and early autumn when nutrient concentrations could increase and peak in riparian sediments and groundwaters with potential implications for water quality management. Low flow and quiescent conditions during late summer or early autumn (July–September) are also generally the preferred time periods for relict dam removals in the US (American Rivers, 2024; Lewis et al., 2021). Our results suggest that the seasonal buildup of NH_4^+ in anaerobic riparian sediments upstream of dams during this period could be a potential N source for downstream waters following dam removal and should be accounted for in dam removal planning.

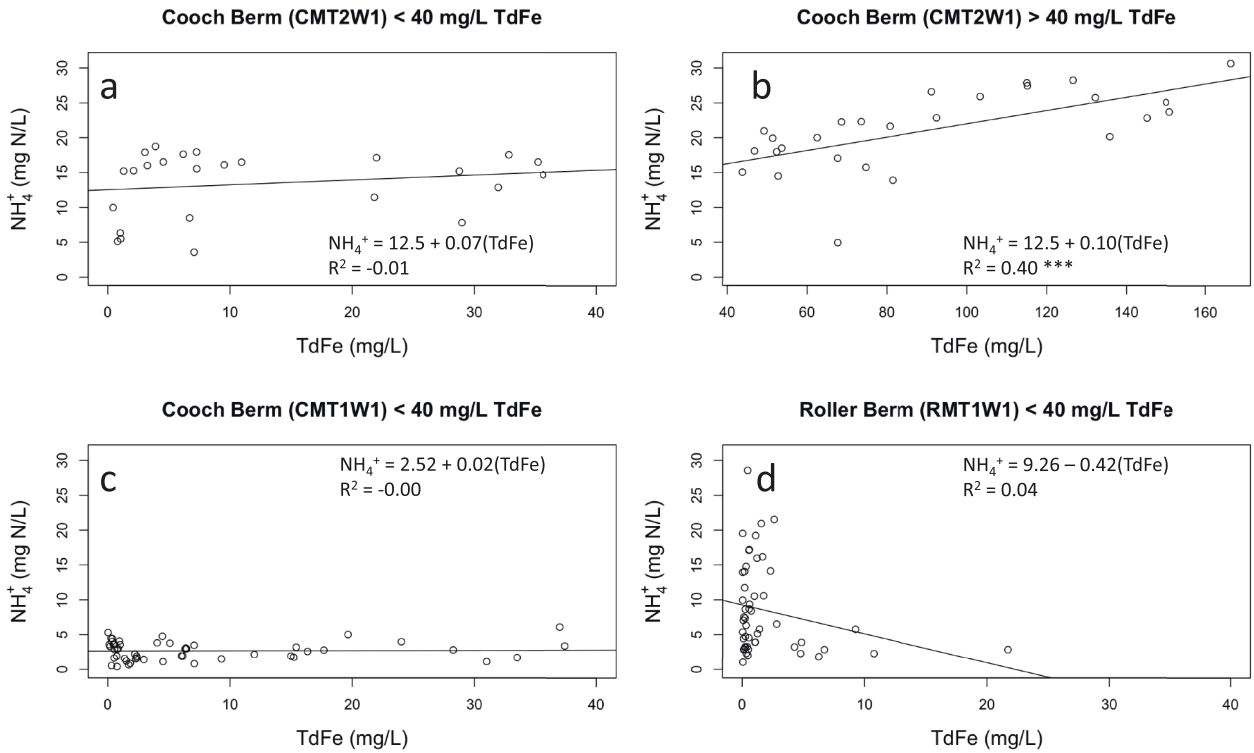

Figure 7. Relationship between TdFe and NH_4^+ concentrations at the CMT2W1 well <40 mg/L (a), and >40 mg/L (b), the CMT1W1 Well <40 mg/L (c), and the RMT1W1 Well <40 mg/L (d). *** = significant slope value (p-value <0.05).

In addition to hydrologic controls, our work also suggests that reducing riparian sediments with elevated lithologic sources of Fe in groundwaters (TdFe >40 mg/L) could serve as hotspots for elevated NH_4^+. Although we attributed the elevated NH_4^+ concentrations to dissimilatory Fe reduction and/or autotrophic DNRA, additional research is needed to verify these mechanisms and the concentrations of Fe that promote these mechanisms. Irrespective of the mechanisms, identification of such "lithologic Fe and NH_4^+ hotspots" should be a priority for water quality management. Aquatic ecosystems and riparian biota could be vulnerable in such settings given that very high concentrations of NH_4^+ in surface and groundwaters are toxic.

Lessons from this study extend beyond riparian zones associated with milldams and could be applicable to other landscape positions that are subject to hydrologic disconnection/stagnation and/or hypoxia/anoxia. These could include storm water ponds or detention basins and/or "accidental wetlands" (Handler et al., 2022) in urban/suburban areas. Similar to our observations, such locations could also become hypoxic/anoxic in hot summer conditions (particularly with extreme climate events, e.g., Inamdar et al., 2017) and result in retention of N. Use of water aerators during such "sensitive" low DO time periods could be one effective mitigation practice to keep waters oxygenated and free of excess NH_4^+.

Data Availability Statement

All water chemistry data used in this manuscript is posted on Zenodo and is publicly available via: https://zenodo.org/records/14582844 and cited below as Sena et al. (2024).

Acknowledgments
We thank the Koser and the Cooch families for permissions to work on their property. This study was funded by the National Science Foundation Hydrologic Sciences Grant 1929747 and 2213855. We also thank Dorothy Merritts, Robert Walter and Jessie Thomas-Blate for their support for the project. Editors and reviewers are also acknowledged for their constructive and careful reviews.

References

American Rivers. (2024). *Dam removal database*. Online. Retrieved from https://figshare.com/articles/dataset/American_Rivers_Dam_Removal_Database/5234068. last accessed 15 January 2025.

An, S., & Gardner, W. S. (2002). Dissimilatory nitrate reduction to ammonium (DNRA) as a nitrogen link, versus denitrification as a sink in a shallow estuary (Laguna Madre/Baffin Bay, Texas). *Marine Ecology Progress Series*, *237*, 41–50. https://doi.org/10.3354/meps237041

Britto, D. T., & Kronzucker, H. J. (2002). NH_4^+ toxicity in higher plants: A critical review. *Journal of Plant Physiology*, *159*(6), 567–584. https://doi.org/10.1078/0176-1617-0774

Chen, Y., Su, X., Wan, Y., Lyu, H., Dong, W., Shi, Y., & Zhang, Y. (2023). Quantifying the effect of the nitrogen biogeochemical processes on the distribution of ammonium in the riverbank filtration system. *Environmental Research*, *216*, 114358. https://doi.org/10.1016/j.envres.2022.114358

Clune, J. W., Capel, P. D., Miller, M. P., Burns, D. A., Sekellick, A. J., Claggett, P., et al. (2019). Nitrogen in the chesapeake bay watershed: A century of change, 1950-2050. *In AGU Fall Meeting Abstracts*, *2019*. GC54D-18.

Covatti, G., & Grischek, T. (2021). Sources and behavior of ammonium during riverbank filtration. *Water Research*, *191*, 116788. https://doi.org/10.1016/j.watres.2020.116788

Dai, Z., Yu, M., Chen, H., Zhao, H., Huang, Y., Su, W., et al. (2020). Elevated temperature shifts soil N cycling from microbial immobilization to enhanced mineralization, nitrification and denitrification across global terrestrial ecosystems. *Global Change Biology*, *26*(9), 5267–5276. https://doi.org/10.1111/gcb.15211

Emsens, W. J., Aggenbach, C. J. S., Schoutens, K., Smolders, A. J. P., Zak, D., & van Diggelen, R. (2016). Soil iron content as a predictor of carbon and nutrient mobilization in rewetted fens. *PLoS One*, *11*(4), e0153166. https://doi.org/10.1371/journal.pone.0153166

Farnsworth, C. E., & Hering, J. G. (2011). Inorganic geochemistry and redox dynamics in bank filtration settings. *Environmental Science and Technology*, *45*(12), 5079–5087. https://doi.org/10.1021/es2001612

Galloway, J. N., Schlesinger, W. H., Levy, H., Michaels, A., & Schnoor, J. L. (1995). Nitrogen fixation: Anthropogenic enhancement-environmental response. *Global Biogeochemical Cycles*, *9*(2), 235–252. https://doi.org/10.1029/95gb00158

Galloway, J. N., Townsend, A. R., Erisman, J. W., Bekunda, M., Cai, Z., Freney, J. R., et al. (2008). Transformation of the nitrogen cycle: Recent trends, questions, and potential solutions. *Science*, *320*(5878), 889–892. https://doi.org/10.1126/science.1136674

Giblin, A. E., Tobias, C. R., Song, B., Weston, N., Banta, G. T., & H. Rivera-Monroy, V. (2013). The importance of dissimilatory nitrate reduction to ammonium (DNRA) in the nitrogen cycle of coastal ecosystems. *Oceanography*, *26*(3), 124–131. https://doi.org/10.5670/oceanog.2013.54

Han, L. L., Wang, H., Ge, L., Xu, M. N., Tang, J. M., Luo, L., et al. (2023). Transition of source/sink processes and fate of ammonium in groundwater along with redox gradients. *Water Research*, *231*, 119600. https://doi.org/10.1016/j.watres.2023.119600

Handler, A. M., Suchy, A. K., & Grimm, N. B. (2022). Denitrification and DNRA in urban accidental wetlands in Phoenix, Arizona. *Journal of Geophysical Research: Biogeosciences*, *127*(2), e2021JG006552. https://doi.org/10.1029/2021jg006552

Harvey, R., Lye, L., Khan, A., & Paterson, R. (2011). The influence of air temperature on water temperature and the concentration of dissolved oxygen in Newfoundland Rivers. *Canadian Water Resources Journal*, *36*(2), 171–192. https://doi.org/10.4296/cwrj3602849

Homer, C. H., & Barnes, C. A. (2012). U.S. Geological Survey fact sheet 2012–3020. *The National Land Cover Database*.

Hripto, J., Inamdar, S., Sherman, M., Peck, E., Gold, A. J., Bernasconi, S., et al. (2022). Effects of relic low-head dams on stream denitrification potential: Seasonality and biogeochemical controls. *Aquatic Sciences*, *84*(4), 60. https://doi.org/10.1007/s00027-022-00894-z

Inamdar, S., Shanley, J. B., & McDowell, W. H. (2017). Aquatic ecosystems in a changing climate. *Eos*, *98*. Published on. https://doi.org/10.1029/2017EO076549 29 June 2017.

Inamdar, S. P., Peck, E. K., Peipoch, M., Sherman, M., Hripto, J., Gold, A. J., et al. (2022). Saturated, suffocated, and salty: Human legacies amplify nitrogen pollution in riparian zones. *Journal of Geophysical Research: Biogeosciences*, *127*(12), e2022JG007138. https://doi.org/10.1029/2022jg007138

Kadlec, R. H., & Reddy, K. R. (2001). Temperature effects in treatment wetlands. *Water Environment Research*, *73*(5), 543–557. https://doi.org/10.2175/106143001x139614

Kaplan, L. A., & Bott, T. L. (1982). Diel fluctuations of DOC generated by algae in a piedmont stream 1. *Limnology & Oceanography*, *27*(6), 1091–1100. https://doi.org/10.4319/lo.1982.27.6.1091

Kresic, N. (2007). Groundwater chemistry. In *Hydrogeology and groundwater modeling*. Taylor and Francis Group.828

Lewis, E., Inamdar, S., Gold, A. J., Addy, K., Trammell, T. L., Merritts, D., et al. (2021). Draining the landscape: How do nitrogen concentrations in riparian groundwater and stream water change following milldam removal? *Journal of Geophysical Research: Biogeosciences*, *126*(8), e2021JG006444. https://doi.org/10.1029/2021jg006444

Liang, Y., Ma, R., Wang, Y., Wang, S., Qu, L., Wei, W., & Gan, Y. (2020). Hydrogeological controls on ammonium enrichment in shallow groundwater in the central Yangtze River Basin. *Science of the Total Environment*, *741*, 140350. https://doi.org/10.1016/j.scitotenv.2020.140350

Mark Jensen, M., Thamdrup, B., Rysgaard, S., Holmer, M., & Fossing, H. (2003). Rates and regulation of microbial iron reduction in sediments of the Baltic-North Sea transition. *Biogeochemistry*, *65*, 295e317.

NOAA. (2021). National Weather Service Forecast Office. Retrieved from https://www.weather.gov/ctp/

Pan, W., Kan, J., Inamdar, S., Chen, C., & Sparks, D. (2016). Dissimilatory microbial iron reduction release DOC (dissolved organic carbon) from carbon-ferrihydrite association. *Soil Biology and Biochemistry*, *103*, 232–240. https://doi.org/10.1016/j.soilbio.2016.08.026

Pandey, C. B., Kumar, U., Kaviraj, M., Minick, K. J., Mishra, A. K., & Singh, J. S. (2020). Dnra: A short-circuit in biological N-cycling to conserve nitrogen in terrestrial ecosystems. *Science of the Total Environment*, *738*, 139710. https://doi.org/10.1016/j.scitotenv.2020.139710

Peck, E. K., Inamdar, S., Sherman, M., Hripto, J., Peipoch, M., Gold, A. J., & Addy, K. (2022). Nitrogen sinks or sources? Denitrification and nitrogen removal potential in riparian legacy sediment terraces affected by milldams. *Journal of Geophysical Research: Biogeosciences*, *127*(10), e2022JG007004. https://doi.org/10.1029/2022jg007004

Rahman, M., Grace, M. R., Roberts, K. L., Kessler, A. J., & Cook, P. L. (2019). Effect of temperature and drying-rewetting of sediments on the partitioning between denitrification and DNRA in constructed urban stormwater wetlands. *Ecological Engineering*, *140*, 105586. https://doi.org/10.1016/j.ecoleng.2019.105586

Rahman, M. M., Peipoch, M., Kan, J., Sena, M., Joshi, B., Dwivedi, D., et al. (2024). Dissimilatory nitrate reduction to ammonium (DNRA) can undermine nitrogen removal effectiveness of persistently reducing riparian sediments. *ACS ES and T Water*, *4*(9), 3873–3881. https://doi.org/10.1021/acsestwater.4c00185

Rahman, M. M., Roberts, K. L., Grace, M. R., Kessler, A. J., & Cook, P. L. (2019). Role of organic carbon, nitrate, and ferrous iron on the partitioning between denitrification and DNRA in constructed stormwater urban wetlands. *Science of the Total Environment*, *666*, 608–617. https://doi.org/10.1016/j.scitotenv.2019.02.225

Ramsey, K. W. (2005). GM13 geologic map of new castle county, Delaware. *Delaware Geological Survey*.

Ranalli, A. J., & Macalady, D. L. (2010). The importance of the riparian zone and in-stream processes in nitrate attenuation in undisturbed and agricultural watersheds—A review of the scientific literature. *Journal of Hydrology*, *389*(3), 406–415. https://doi.org/10.1016/j.jhydrol.2010.05.045

Reddy, K. R., DeLaune, R. D., & Inglett, P. W. (2022). *Biogeochemistry of wetlands: Science and applications*. CRC press.

Riedel, T. (2019). Temperature-associated changes in groundwater quality. *Journal of Hydrology*, *572*, 206–212. https://doi.org/10.1016/j.jhydrol.2019.02.059

Robertson, E. K., Roberts, K. L., Burdorf, L. D., Cook, P., & Thamdrup, B. (2016). Dissimilatory nitrate reduction to ammonium coupled to Fe (II) oxidation in sediments of a periodically hypoxic estuary. *Limnology & Oceanography*, *61*(1), 365–381. https://doi.org/10.1002/lno.10220

Robertson, E. K., & Thamdrup, B. (2017). The fate of nitrogen is linked to iron (II) availability in a freshwater lake sediment. *Geochimica et Cosmochimica Acta*, *205*, 84–99. https://doi.org/10.1016/j.gca.2017.02.014

Rubol, S., Manzoni, S., Bellin, A., & Porporato, A. (2013). Modeling soil moisture and oxygen effects on soil biogeochemical cycles including dissimilatory nitrate reduction to ammonium (DNRA). *Advances in Water Resources*, *62*, 106–124. https://doi.org/10.1016/j.advwatres.2013.09.016

Rütting, T., Boeckx, P., Müller, C., & Klemedtsson, L. (2011). Assessment of the importance of dissimilatory nitrate reduction to ammonium for the terrestrial nitrogen cycle. *Biogeosciences*, *8*(7), 1779–1791. https://doi.org/10.5194/bg-8-1779-2011

Sahrawat, K. L. (2004). Ammonium production in submerged soils and sediments: The role of reducible iron. *Communications in Soil Science and Plant Analysis*, *35*(3–4), 399–411. https://doi.org/10.1081/css-120029721

Sena, M., Peipoch, M., Joshi, B., Rahman, M., Peck, E., Gold, A. J., et al. (2024). Seasonal variation and key controls of groundwater ammonium concentrations in hypoxic/anoxic riparian sediments. *Zenodo*. [Dataset]. https://doi.org/10.5281/zenodo.14582844

Sherman, M., Hripto, J., Peck, E. K., Gold, A. J., Peipoch, M., Imhoff, P., & Inamdar, S. (2022). Backed-up, saturated, and stagnant: Effect of milldams on upstream riparian groundwater hydrologic and mixing regimes. *Water Resources Research*, *58*(10), e2022WR033038. https://doi.org/10.1029/2022wr033038

Singh, R., Tiwari, A. K., & Singh, G. S. (2021). Managing riparian zones for river health improvement: An integrated approach. *Landscape and Ecological Engineering*, *17*(2), 195–223. https://doi.org/10.1007/s11355-020-00436-5

Soil Survey. (2021). *Web soil Survey. Natural resources conservation Service*. United States Department of Agriculture. Retrieved from http://websoilsurvey.sc.egov.usda.gov/

Thamdrup, B. (2000). Bacterial manganese and iron reduction in aquatic sediments. In B. Schink (Ed.), *Advances in microbial ecology* (p. 41e84). Springer.

Tiedje, J. M. (1988). Ecology of denitrification and dissimilatory nitrate reduction to ammonium. *Biology of Anaerobic Microorganisms*, 179–244.

Vitousek, P. M., Mooney, H. A., Lubchenco, J., & Melillo, J. M. (1997). Human domination of Earth's ecosystems. *Science*, *277*(5325), 494–499. https://doi.org/10.1126/science.277.5325.494

Wang, S., Pi, Y., Song, Y., Jiang, Y., Zhou, L., Liu, W., & Zhu, G. (2020). Hotspot of dissimilatory nitrate reduction to ammonium (DNRA) process in freshwater sediments of riparian zones. *Water Research*, *173*, 115539. https://doi.org/10.1016/j.watres.2020.115539

Wei, Z., Jin, K., Li, C., Wu, M., Shan, J., & Yan, X. (2022). Environmental factors controlling dissimilatory nitrate reduction to ammonium in paddy soil. *Journal of Soil Science and Plant Nutrition*, *22*(4), 1–8. https://doi.org/10.1007/s42729-022-01022-4

Yang, X. E., Wu, X., Hao, H. L., & He, Z. L. (2008). Mechanisms and assessment of water eutrophication. *Journal of Zhejiang University - Science B*, *9*(3), 197–209. https://doi.org/10.1631/jzus.b0710626

Yuan, H., Cai, Y., Wang, H., Liu, E., & Zeng, Q. (2023). Impact of seasonal change on dissimilatory nitrate reduction to ammonium (DNRA) triggering the retention of nitrogen in lake. *Journal of Environmental Management*, *341*, 118050. https://doi.org/10.1016/j.jenvman.2023.118050

Zhang, X., Ren, P., Zhou, J., Li, J., Li, Z., & Wang, D. (2022). Formation of disinfection byproducts in an ammonia-polluted source water with UV/chlorine treatment followed by post-chlorination: A pilot-scale study. *Environmental Technology and Innovation*, *26*, 102266. https://doi.org/10.1016/j.eti.2021.102266

Zhang, X., Ward, B. B., & Sigman, D. M. (2020). Global nitrogen cycle: Critical enzymes, organisms, and processes for nitrogen budgets and dynamics. *Chemical Reviews*, *120*(12), 5308–5351. https://doi.org/10.1021/acs.chemrev.9b00613

Zhao, S., Zhang, B., & Zhou, N. (2020). Effects of redox potential on the environmental behavior of nitrogen in riparian zones of West Dongting Lake Wetlands, China. *Wetlands*, *40*(5), 1307–1316. https://doi.org/10.1007/s13157-020-01301-9